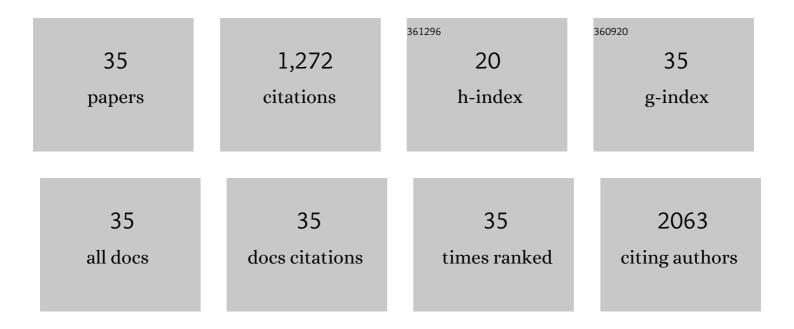


List of Publications by Year in descending order

Source: https://exaly.com/author-pdf/9113740/publications.pdf Version: 2024-02-01



\\/ELL

#	Article	IF	CITATIONS
1	Enhanced Photocatalytic Activity in Anatase/TiO ₂ (B) Coreâ^'Shell Nanofiber. Journal of Physical Chemistry C, 2008, 112, 20539-20545.	1.5	181
2	Highly Thermal Stable and Highly Crystalline Anatase TiO ₂ for Photocatalysis. Environmental Science & Technology, 2009, 43, 5423-5428.	4.6	103
3	Microencapsulated Phase Change Materials in Solar-Thermal Conversion Systems: Understanding Geometry-Dependent Heating Efficiency and System Reliability. ACS Nano, 2017, 11, 721-729.	7.3	98
4	Core–shell TiO2/C nanofibers as supports for electrocatalytic and synergistic photoelectrocatalytic oxidation of methanol. Journal of Materials Chemistry, 2012, 22, 4025.	6.7	83
5	Stability of Pt nanoparticles and enhanced photocatalytic performance in mesoporous Pt-(anatase/TiO2(B)) nanoarchitecture. Journal of Materials Chemistry, 2009, 19, 7055.	6.7	72
6	Pyrite nanocrystals: shape-controlled synthesis and tunable optical properties via reversible self-assembly. Journal of Materials Chemistry, 2011, 21, 17946.	6.7	72
7	One-step electrochemical synthesis of a graphene–ZnO hybrid for improved photocatalytic activity. Materials Research Bulletin, 2013, 48, 2855-2860.	2.7	66
8	Template free mild hydrothermal synthesis of core–shell Cu ₂ O(Cu)@CuO visible light photocatalysts for <i>N</i> -acetyl- <i>para</i> -aminophenol degradation. Journal of Materials Chemistry A, 2019, 7, 20767-20777.	5.2	46
9	Size-dependent electroluminescence from Si quantum dots embedded in amorphous SiC matrix. Journal of Applied Physics, 2011, 110, .	1.1	45
10	Structural and electronic properties of Si nanocrystals embedded in amorphous SiC matrix. Journal of Alloys and Compounds, 2011, 509, 3963-3966.	2.8	43
11	Excellent performance of Pt-C/TiO 2 for methanol oxidation: Contribution of mesopores and partially coated carbon. Applied Surface Science, 2017, 426, 890-896.	3.1	38
12	A shortcut for evaluating activities of TiO2 facets: water dissociative chemisorption on TiO2-B (100) and (001). Physical Chemistry Chemical Physics, 2010, 12, 8721.	1.3	37
13	Synthesis, Features, and Applications of Mesoporous Titania with TiO2(B). Chinese Journal of Catalysis, 2010, 31, 605-614.	6.9	36
14	Single-crystalline and reactive facets exposed anatase TiO2 nanofibers with enhanced photocatalytic properties. Journal of Materials Chemistry, 2011, 21, 6718.	6.7	31
15	Novel mesoporous TiO2(B) whisker-supported sulfated solid superacid with unique acid characteristics and catalytic performances. Applied Catalysis A: General, 2019, 574, 25-32.	2.2	31
16	Joint Event Extraction Based on Hierarchical Event Schemas From FrameNet. IEEE Access, 2019, 7, 25001-25015.	2.6	26
17	Low-Temperature CO Oxidation of Gold Catalysts Loaded on Mesoporous TiO2 Whisker Derived from Potassium Dititanate. Catalysis Letters, 2009, 127, 406-410.	1.4	23
18	Highly Crystalline Mesoporous TiO ₂ (B) Nanofibers. Journal of Physical Chemistry C, 2014, 118, 3049-3055.	1.5	21

Wei Li

#	Article	IF	CITATIONS
19	Simultaneous Optimization of Colloidal Stability and Interfacial Charge Transfer Efficiency in Photocatalytic Pt/CdS Nanocrystals. ACS Applied Materials & Interfaces, 2016, 8, 29434-29441.	4.0	20
20	TiO ₂ Nanofoam–Nanotube Array for Surface-Enhanced Raman Scattering. ACS Applied Nano Materials, 2018, 1, 6563-6566.	2.4	20
21	Size-controlled electron transfer rates determine hydrogen generation efficiency in colloidal Pt-decorated CdS quantum dots. Nanoscale, 2018, 10, 16153-16158.	2.8	19
22	Comparative Study in Liquid-Phase Heterogeneous Photocatalysis: Model for Photoreactor Scale-Up. Industrial & Engineering Chemistry Research, 2010, 49, 8397-8405.	1.8	18
23	Mitigating air pollution strategies based on solar chimneys. Solar Energy, 2021, 218, 11-27.	2.9	18
24	In-situ synthesized mesoporous TiO2-B/anatase microparticles: Improved anodes for lithium ion batteries. Chinese Journal of Chemical Engineering, 2015, 23, 583-589.	1.7	17
25	Optical and Electronic Properties of Pyrite Nanocrystal Thin Films: the Role of Ligands. Small, 2014, 10, 1194-1201.	5.2	16
26	Hydrophilic, Hole-Delocalizing Ligand Shell to Promote Charge Transfer from Colloidal CdSe Quantum Dots in Water. Journal of Physical Chemistry C, 2017, 121, 15160-15168.	1.5	16
27	Nanolamellar Tantalum Interfaces in the Osteoblast Adhesion. Langmuir, 2019, 35, 2480-2489.	1.6	16
28	Colloidal dual-band gap cell for photocatalytic hydrogen generation. Nanoscale, 2015, 7, 16606-16610.	2.8	12
29	Enhanced green to red photoluminescence in thermally annealed of amorphous-Si:H/SiO2 multilayers. Thin Solid Films, 2006, 515, 2322-2325.	0.8	11
30	Luminescence behavior from amorphous silicon-carbide film-based optical microcavities. Materials Chemistry and Physics, 2008, 111, 279-282.	2.0	11
31	Effects of ionic hydration and hydrogen bonding on flow resistance of ionic aqueous solutions confined in molybdenum disulfide nanoslits: Insights from molecular dynamics simulations. Fluid Phase Equilibria, 2019, 489, 23-29.	1.4	9
32	Thermodynamic Analysis on the Mineralization of Trace Organic Contaminants with Oxidants in Advanced Oxidation Processes. Industrial & Engineering Chemistry Research, 2009, 48, 10728-10733.	1.8	6
33	Nanowhiskers of K2Ti6O13 as a promoter of photocatalysis in anatase mesocrystals. Catalysis Today, 2021, 378, 133-139.	2.2	5
34	Nanopatterned surface with adjustable area coverage and feature size fabricated by photocatalysis. Applied Surface Science, 2009, 255, 9296-9300.	3.1	4
35	Highly Crystalline TiO ₂ Whisker Modified with Pt and Its Photocata-lytic Performance. Chinese Journal of Catalysis, 2010, 31, 1271-1276.	6.9	2